

Analysis of a thickness-shear piezoelectric transformer

J.S. Yang and X. Zhang

Department of Engineering Mechanics, University of Nebraska, Lincoln, NE 68588, USA

Abstract. A theoretical analysis is performed on a high voltage piezoelectric transformer operating with thickness-shear modes using the zero-dimensional equations of a piezoelectric parallelepiped. Analytical solutions for the transforming ratio and efficiency of the transformer are obtained. Their dependence on the driving frequency, load impedance and geometric parameters are examined.

1. Introduction

Piezoelectric materials can be used to make transformers of various designs [1–4]. They can be classified as low or high voltage transformers. A high voltage piezoelectric transformer works with two characteristic lengths, one is small and the other is large. The transformer is driven into mechanical vibration at its driving portion by an applied voltage across the smaller characteristic length, so that a low driving voltage can generate a reasonably strong electric field and the accompanying mechanical field through the piezoelectric effect. This mechanical field propagates into the receiving portion of the transformer and produces an electric field and hence voltage there, again because the material is piezoelectric. For high voltage transformers this voltage accumulates spatially in the receiving portion and is picked up by electrodes across the larger characteristic length of the transformer. The traditional high voltage transformer is the Rosen transformer [1] working with extensional vibration modes of a rod. A low voltage transformer works with the small characteristic length at both the driving and receiving portions. Examples are the thickness extension mode of a plate [2], Lamé mode of a plate [3], or shear mode of a plate or beam [4].

A high voltage piezoelectric transformer operating with thickness-shear modes was proposed in [5]. When made of ceramics, the thickness-shear high voltage transformer suggested in [5] works with the piezoelectric constant d_{15} , while the conventional extensional high voltage transformer uses d_{31} and d_{33} . For commonly used ceramics, d_{15} is much larger than d_{31} or d_{33} in value [6]. Hence more effective transforming can be expected for the ceramic thickness-shear transformers suggested in [5] than the common Rosen type ceramic extensional transformers. Rosen transformers using longitudinal extension modes are mounted at the nodal points of the extensional modes. Theoretically, mounting at nodal points will not affect the performance of the transformer. In reality this is difficult to achieve because any mounting will actually occupy a small area around the nodal point. Furthermore, the exact locations of nodal points are in fact changing when the transformer is working under different driving and loading conditions. Thickness-shear transformers can be mounted in a different way by the energy-trapping technique [7]. With the Energy-trapping technique, the thickness-shear vibration of the transformer can

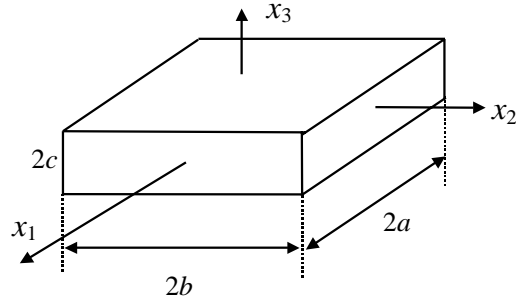


Fig. 1. A rectangular parallelepiped.

be confined in one portion of the transformer and in the rest of the transformer there is no shear motion. In this region without motion, the transformer can be mounted without affecting its vibration.

The major characteristics of a piezoelectric transformer can be obtained from an analysis based on the linear theory of piezoelectricity. A piezoelectric free vibration analysis was performed in [5] on the thickness-shear high voltage piezoelectric transformer suggested. Free vibration frequency equation and modes were obtained. The purpose of the free vibration analysis is to analytically exhibit the mechanism of the transformer by showing the operating modes.

Recently, zero-dimensional equations for motions of a piezoelectric parallelepiped were derived in [8] from the three-dimensional equations of piezoelectricity. These equations represent a generalization of the zero-dimensional equations of an elastic body [9]. The zero-dimensional equations obtained in [8] are ordinary differential equations with time as the only independent variable, which are the simplest model of a deformable body and are convenient for theoretical analysis because of their simplicity. The equations in [8] can be used to model the motion and deformation of a piezoelectric body in any particular vibration or deformation mode. The lowest order equations for homogeneous deformations and uniform electric fields have been used to model a ceramic thickness-shear piezoelectric gyroscope [8]. Many piezoelectric components used as transducers, resonators or sensors are piezoelectric bodies in single-mode vibrations which can be very well modeled by the zero-dimensional theory. For designs of many piezoelectric devices the global behavior like the transforming ratio or input-output powers are of main interest. For these purposes the zero-dimensional equations which are in terms of averaged quantities can lead to simple and useful results.

In this paper we perform a forced vibration analysis of the transformer in [5] under a time-harmonic driving voltage. The analysis is based on the zero-dimensional equations of a piezoelectric parallelepiped. The transformer will be treated as two connected piezoelectric parallelepipeds, one represent the driving portion and the other the receiving portion. Equations for the whole transformer are obtained using the continuity conditions between the two portions. Simple analytical solutions are obtained showing the basic behaviors of the transformer.

2. Equations for a piezoelectric parallelepiped

The three-dimensional equations for linear piezoelectricity can be written as [10]

$$\begin{aligned} T_{ji,j} + \rho f_i &= \rho \ddot{u}_i, & D_{i,i} &= 0, \\ T_{ij} &= c_{ijkl} S_{kl} - e_{kij} E_k, & D_i &= e_{ijk} S_{jk} + \varepsilon_{ij}^S E_j, \end{aligned} \quad (1)$$

$$S_{ij} = \frac{1}{2}(u_{i,j} + u_{j,i}), \quad E_i = -\phi_{,i},$$

where u_i is the mechanical displacement vector, T_{ij} the stress tensor, S_{ij} the strain tensor, E_i the electric field, D_i the electric displacement, and ϕ the electric potential. ε_{ijk} is the permutation tensor. c_{ijkl} , e_{kij} and ε_{ij}^S are the elastic, piezoelectric and dielectric constants. ρ is the mass density, and f_i the body force. Equations in Eq. (1) are the balance of linear momentum, electrostatics, mechanical and electric constitutive relations, strain-displacement relation and electric field-potential relation, respectively. Summation convention for repeated tensor indices and the convention that a comma followed by an index denotes partial differentiation with respect to the coordinate associated with the index are used. A superimposed dot represents time derivative. On the boundary of a finite piezoelectric body, usually the mechanical displacement u_i or the traction vector $T_{ji}n_j$, and the electric potential ϕ or the normal component of the electric displacement vector $D_i n_i$ are prescribed. Very often, constitutive relations of the following form are more convenient.

$$S_{ij} = s_{ijkl}T_{kl} + d_{kij}E_k, \quad D_i = d_{ijk}T_{jk} + \varepsilon_{ij}^T E_j. \quad (2)$$

Consider a piezoelectric rectangular parallelepiped as shown in Fig. 1. The zero-dimensional theory is based on the following expansions of the three-dimensional mechanical displacement vector and the electrostatic potential [8].

$$u_j(x_1, x_2, x_3, t) = \sum_{l,m,n=0}^{\infty} x_1^l x_2^m x_3^n u_j^{(l,m,n)}(t), \quad (3)$$

$$\phi(x_1, x_2, x_3, t) = \sum_{l,m,n=0}^{\infty} x_1^l x_2^m x_3^n \phi^{(l,m,n)}(t).$$

Substitution of Eq. (3) into the variational formulation [10] of the three-dimensional theory of piezoelectricity leads to the zero-dimensional equations of a piezoelectric parallelepiped. The lowest order equations of motion and electrostatics corresponding to $(l, m, n) = (0,0,0), (1,0,0), (0,1,0)$ and $(0,0,1)$ are [8].

$$F_j^{(0,0,0)} = \rho 8abc \ddot{u}_j^{(0,0,0)}, \quad (4)$$

$$D^{(0,0,0)} = 0,$$

$$-T_{1j}^{(0,0,0)} + F_j^{(1,0,0)} = \rho \frac{8a^3bc}{3} \ddot{u}_j^{(1,0,0)}, \quad (5)$$

$$-D_1^{(0,0,0)} + D^{(1,0,0)} = 0,$$

$$-T_{2j}^{(0,0,0)} + F_j^{(0,1,0)} = \rho \frac{8ab^3c}{3} \ddot{u}_j^{(0,1,0)}, \quad (6)$$

$$-D_2^{(0,0,0)} + D^{(0,1,0)} = 0,$$

$$-T_{3j}^{(0,0,0)} + F_j^{(0,0,1)} = \rho \frac{8abc^3}{3} \ddot{u}_j^{(0,0,1)}, \quad (7)$$

$$-D_3^{(0,0,0)} + D^{(0,0,1)} = 0,$$

where the zero-dimensional stress resultants and the electric displacement resultants are defined by

$$T_{ij}^{(0,0,0)} = \int_V T_{ij} dV, \quad D_i^{(0,0,0)} = \int_V D_i dV. \quad (8)$$

In Eq. (8), $V = 8abc$ is the volume of the parallelepiped. Surface traction, surface charge and body force of various orders are defined by

$$\begin{aligned} F_j^{(l,m,n)} &= T_j^{(l,m,n)} + \rho f_j^{(l,m,n)}, \\ T_j^{(l,m,n)} &= \int_{-b}^b dx_2 \int_{-c}^c dx_3 [T_{1j}(a) - (-1)^l T_{1j}(-a)] a^l x_2^m x_3^n \\ &\quad + \int_{-a}^a dx_1 \int_{-c}^c dx_3 [T_{2j}(b) - (-1)^m T_{2j}(-b)] b^m x_1^l x_3^n \\ &\quad + \int_{-a}^a dx_1 \int_{-b}^b dx_2 [T_{3j}(c) - (-1)^n T_{3j}(-c)] c^n x_1^l x_2^m, \quad f_j^{(l,m,n)} = \int_V x_1^l x_2^m x_3^n f_j dV, \end{aligned} \quad (9)$$

$$\begin{aligned} D^{(l,m,n)} &= \int_{-b}^b dx_2 \int_{-c}^c dx_3 [D_1(a) - (-1)^l D_1(-a)] a^l x_2^m x_3^n \\ &\quad + \int_{-a}^a dx_1 \int_{-c}^c dx_3 [D_2(b) - (-1)^m D_2(-b)] b^m x_1^l x_3^n \\ &\quad + \int_{-a}^a dx_1 \int_{-b}^b dx_2 [D_3(c) - (-1)^n D_3(-c)] c^n x_1^l x_2^m. \end{aligned} \quad (10)$$

Constitutive relations for the above equations are given by [8].

$$\begin{aligned} T_M^{(0,0,0)} &= 8abc(c_{MN} S_N^{(0,0,0)} - e_{kM} E_k^{(0,0,0)}) \\ D_i^{(0,0,0)} &= 8abc(e_{iN} S_N^{(0,0,0)} + \varepsilon_{ik} E_k^{(0,0,0)}), \end{aligned} \quad (11)$$

where the compact matrix notation [10] for the three-dimensional elastic, piezoelectric, and dielectric tensors c_{ijkl} , e_{kij} , and ε_{ij} are used with $M, N = 1, 2, \dots, 6$. The lowest order strains and electric fields are given by

$$\begin{aligned} S_1^{(0,0,0)} &= u_1^{(1,0,0)}, \quad S_4^{(0,0,0)} = u_2^{(0,0,1)} + u_3^{(0,1,0)}, \\ S_2^{(0,0,0)} &= u_2^{(0,1,0)}, \quad S_5^{(0,0,0)} = u_3^{(1,0,0)} + u_1^{(0,0,1)}, \\ S_3^{(0,0,0)} &= u_3^{(0,0,1)}, \quad S_6^{(0,0,0)} = u_1^{(0,1,0)} + u_2^{(1,0,0)}, \end{aligned} \quad (12)$$

$$E_1^{(0,0,0)} = -\phi^{(1,0,0)}, \quad E_2^{(0,0,0)} = -\phi^{(0,1,0)}, \quad E_3^{(0,0,0)} = -\phi^{(0,0,1)}. \quad (13)$$

With successive substitutions, the above equations can be written as equations for $u_j^{(0,0,0)}$, $u_j^{(1,0,0)}$, $u_j^{(0,1,0)}$, $u_j^{(0,0,1)}$, $\phi^{(1,0,0)}$, $\phi^{(0,1,0)}$, and $\phi^{(0,0,1)}$ which govern the rigid body motion and homogeneous deformation of the parallelepiped with uniform electric fields.

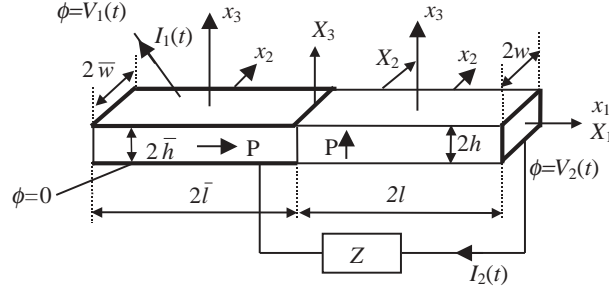


Fig. 2. A thickness-shear high voltage piezoelectric transformer.

3. Equations for the transformer

Consider the piezoelectric transformer shown in Fig. 2. It is assumed that $l, \bar{l} \gg w, \bar{w} \gg h, \bar{h}$. The driving portion $-\bar{l} < X_1 < 0$ is electroded at $x_3 = \pm \bar{h}$, with electrodes in the areas bounded by the thick lines. In the receiving portion $0 < X_1 < l$, the beam is electroded at the end $X_1 = l$. The driving portion and the receiving portion may have slightly different thickness $2\bar{h}$ and $2h$, and width $2\bar{w}$ and $2w$. V_1 is the input voltage and V_2 the output voltage. When it is made of polarized ceramics, the polarization in the driving and receiving portions are as shown. For each portion of the transformer there exists a local Cartesian coordinate system x_i with its origin at the center of the portion and directions along the global system X_i . The thickness-shear motion we are considering can be approximately represented by

$$u_1 \cong x_3 u_1^{(0,0,1)}, \quad u_2 \cong 0, \quad u_3 \cong 0. \tag{14}$$

In the driving portion the electric potential is the known driving potential with

$$\phi \cong \phi^{(0,0,0)} + x_3 \phi^{(0,0,1)}, \quad \phi^{(0,0,0)} = V_1/2, \phi^{(0,0,1)} = V_1/(2\bar{h}). \tag{15}$$

In the receiving portion the electric potential can be written as

$$\phi \cong \phi^{(0,0,0)} + x_1 \phi^{(1,0,0)}, \quad \phi^{(0,0,0)} = V_2/2, \phi^{(1,0,0)} = V_2/(2l), \tag{16}$$

where V_2 is unknown.

3.1. Equations for the receiving portion

Ceramics poled in the X_3 direction are transversely isotropic in the $X_1 - X_2$ plane with material matrices given by [6]

$$\begin{pmatrix} c_{11} & c_{12} & c_{13} & 0 & 0 & 0 \\ c_{21} & c_{11} & c_{13} & 0 & 0 & 0 \\ c_{31} & c_{31} & c_{33} & 0 & 0 & 0 \\ 0 & 0 & 0 & c_{44} & 0 & 0 \\ 0 & 0 & 0 & 0 & c_{44} & 0 \\ 0 & 0 & 0 & 0 & 0 & c_{66} \end{pmatrix}, \begin{pmatrix} 0 & 0 & e_{31} \\ 0 & 0 & e_{31} \\ 0 & 0 & e_{33} \\ 0 & e_{15} & 0 \\ e_{15} & 0 & 0 \\ 0 & 0 & 0 \end{pmatrix}, \begin{pmatrix} \varepsilon_{11} & 0 & 0 \\ 0 & \varepsilon_{11} & 0 \\ 0 & 0 & \varepsilon_{33} \end{pmatrix}. \tag{17}$$

The equation for the shear motion $u_1^{(0,0,1)}$ can be obtained from Eq. (7)₁ by setting $j = 1$

$$-T_{31}^{(0,0,0)} + F_1^{(0,0,1)} = \rho \frac{8lwh^3}{3} \ddot{u}_1^{(0,0,1)}, \tag{18}$$

where, from Eq. (9)

$$F_1^{(0,0,1)} = \int_{-w}^w \int_{-h}^h -T_{11}(X_1 = 0^+) X_3 dX_2 dX_3. \quad (19)$$

In obtaining Eq. (19), we have assumed that there is no body force and made use of the traction free boundary conditions at $X_1 = 2l$, $X_2 = \pm w$, and $X_3 = \pm h$. Relevant constitutive relations take the following form from Eq. (11)

$$\begin{aligned} T_{31}^{(0,0,0)} &= 8lwh(c_{44}\kappa^2 S_5^{(0,0,0)} - e_{15}\kappa E_1^{(0,0,0)}), \\ D_1^{(0,0,0)} &= 8lwh(e_{15}\kappa S_5^{(0,0,0)} + \varepsilon_{11} E_1^{(0,0,0)}). \end{aligned} \quad (20)$$

In Eq. (20) we have introduced a thickness-shear correction factor κ in the manner of Mindlin [11] to compensate the error caused by truncating the series expansions in obtaining the zero-dimensional equations. For a ceramic parallelepiped we have $\kappa^2 = \pi^2/12$. The total electric charge on the electrode at $X_1 = 2l$ and the electric current flows out of the electrode are given by

$$Q_2 = -D_1^{(0,0,0)}/(2l), \quad I_2 = -\dot{Q}_2. \quad (21)$$

3.2. Equations for the driving portion

For ceramics poled in the X_1 direction, the material matrices can be obtained by reordering rows and columns of the matrices in Eq. (22), with the result

$$\begin{pmatrix} c_{33} & c_{13} & c_{13} & 0 & 0 & 0 \\ c_{13} & c_{11} & c_{12} & 0 & 0 & 0 \\ c_{13} & c_{12} & c_{11} & 0 & 0 & 0 \\ 0 & 0 & 0 & c_{66} & 0 & 0 \\ 0 & 0 & 0 & 0 & c_{44} & 0 \\ 0 & 0 & 0 & 0 & 0 & c_{44} \end{pmatrix}, \begin{pmatrix} e_{33} & 0 & 0 \\ e_{31} & 0 & 0 \\ e_{31} & 0 & 0 \\ 0 & 0 & 0 \\ 0 & 0 & e_{15} \\ 0 & e_{15} & 0 \end{pmatrix}, \begin{pmatrix} \varepsilon_{33} & 0 & 0 \\ 0 & \varepsilon_{11} & 0 \\ 0 & 0 & \varepsilon_{11} \end{pmatrix}. \quad (22)$$

The equation of motion is

$$-T_{31}^{(0,0,0)} + F_1^{(0,0,1)} = \rho \frac{8\bar{l}\bar{w}\bar{h}^3}{3} \ddot{u}_1^{(0,0,1)}, \quad (23)$$

where

$$F_1^{(0,0,1)} = \int_{-\bar{w}}^{\bar{w}} \int_{-\bar{h}}^{\bar{h}} T_{11}(X_1 = 0^-) X_3 dX_2 dX_3. \quad (24)$$

The constitutive relations are

$$\begin{aligned} T_{31}^{(0,0,0)} &= 8\bar{l}\bar{w}\bar{h}(c_{44}\kappa^2 S_5^{(0,0,0)} - e_{15}\kappa E_3^{(0,0,0)}), \\ D_3^{(0,0,0)} &= 8\bar{l}\bar{w}\bar{h}(e_{15}\kappa S_5^{(0,0,0)} + \varepsilon_{11} E_3^{(0,0,0)}). \end{aligned} \quad (25)$$

For the charge and current on the electrode at $X_3 = \bar{h}$ we have

$$Q_1 = -D_3^{(0,0,0)}/(2\bar{h}), \quad I_1 = -\dot{Q}_1. \quad (26)$$

3.3. Equations for the whole transformer

Substituting Eq. (20)₁ into Eq. (18), and Eq. (25)₁ into Eq. (23), adding the resulting equations and making use of Eq. (14)₁ and the continuity conditions

$$T_{11}(X_1 = 0^-) = T_{11}(X_1 = 0^+), u_1(X_1 = 0^-) = u_1(X_1 = 0^+), \quad (27)$$

We obtain

$$\begin{aligned} & -8lwh(c_{44}\kappa^2 S_5^{(0,0,0)} - e_{15}\kappa E_1^{(0,0,0)}) - 8\bar{l}\bar{w}\bar{h}(c_{44}\kappa^2 S_5^{(0,0,0)} - e_{15}\kappa E_3^{(0,0,0)}) \\ & = 8/3\rho(lwh^3 + \bar{l}\bar{w}\bar{h}^3)\ddot{u}_1^{(0,0,1)}. \end{aligned} \quad (28)$$

Under known time-harmonic driving voltage $V_1 = \bar{V}_1 e^{i\omega t}$, for time-harmonic solutions we employ the complex notation and write the unknowns as

$$u_1^{(0,0,1)} = \bar{u} e^{i\omega t}, V_2 = \bar{V}_2 e^{i\omega t}, I_1 = \bar{I}_1 e^{i\omega t}, I_2 = \bar{I}_2 e^{i\omega t}. \quad (29)$$

The receiving electrodes are usually connected by an output circuit which, when the motion is time-harmonic, has an impedance Z_L . In the special cases when $Z_L = 0$ or ∞ we have short or open output circuit with $V_2 = 0$ or $I_2 = 0$. In general neither V_2 nor I_2 are known and we have the following circuit condition.

$$\bar{I}_2 = \bar{V}_2 / Z_L. \quad (30)$$

Then, from Eq. (28) and Eq. (30), with the use of Eqs (12), (13), (15), (16), (20)₂, (21) and (29), we obtain the following two equations for \bar{u} and \bar{V}_2 , driven by \bar{V}_1 .

$$\begin{aligned} & -8lwh \left(c_{44}\kappa^2 \bar{u} + e_{15}\kappa \frac{\bar{V}_2}{2l} \right) - 8\bar{l}\bar{w}\bar{h} \left(c_{44}\kappa^2 \bar{u} + e_{15}\kappa \frac{\bar{V}_1}{2\bar{h}} \right) \\ & = -\frac{8}{3}\rho(lwh^3 + \bar{l}\bar{w}\bar{h}^3)\omega^2 \bar{u}, 4whi\omega \left(e_{15}\kappa \bar{u} - \varepsilon_{11} \frac{\bar{V}_2}{2l} \right) = \frac{\bar{V}_2}{Z_L}. \end{aligned} \quad (31)$$

Once \bar{u} and \bar{V}_2 are obtained from Eq. (31), we can obtain, from Eqs (20)₂, (21), (25)₂ and (26).

$$\bar{I}_2 = 4whi\omega \left(e_{15}\kappa \bar{u} - \varepsilon_{11} \frac{\bar{V}_2}{2l} \right), \bar{I}_1 = 4\bar{l}\bar{w}i\omega \left(e_{15}\kappa \bar{u} - \varepsilon_{11} \frac{\bar{V}_1}{2\bar{h}} \right). \quad (32)$$

4. Forced vibration analysis

We consider the case of $l = \bar{l}$ and $w = \bar{w}$. Solving Eq. (31) for \bar{u} and \bar{V}_2 , substituting the results into Eq. (32), we obtain the transforming ratio and normalized input and output currents as

$$\begin{aligned} \frac{\bar{V}_2}{\bar{V}_1} &= \frac{k_{15}^2}{(1 + h/\bar{h})(1 + Z_2/Z_L)(\omega^2/\omega_0^2 - 1) - k_{15}^2 h/\bar{h}} \frac{l}{\bar{h}}, \\ \frac{\bar{I}_2}{(\bar{V}_1/Z_2)} &= \frac{k_{15}^2}{(1 + h/\bar{h})(1 + Z_L/Z_2)(\omega^2/\omega_0^2 - 1) - k_{15}^2 h Z_L/(\bar{h} Z_2)} \frac{l}{\bar{h}}, \\ -\frac{\bar{I}_1}{(\bar{V}_1/Z_1)} &= 1 - \frac{k_{15}^2(1 + Z_2/Z_L)}{(1 + h/\bar{h})(1 + Z_2/Z_L)(\omega^2/\omega_0^2 - 1) - k_{15}^2 h/\bar{h}}, \end{aligned} \quad (33)$$

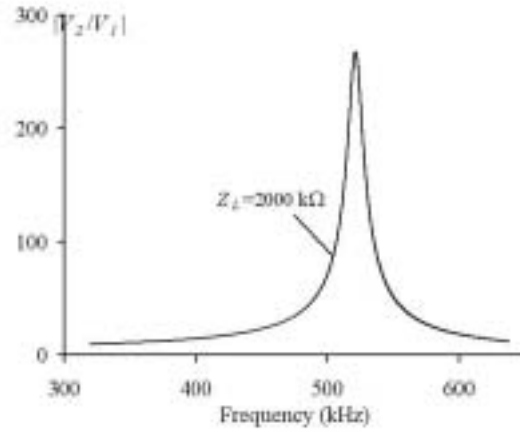


Fig. 3. Transforming ratio versus driving frequency.

where

$$\begin{aligned}
 k_{15}^2 &= \frac{e_{15}^2}{\varepsilon_{11}c_{44}}, & \omega_0^2 &= \frac{3\kappa^2c_{44}}{\rho(h^2 - h\bar{h} + \bar{h}^2)}, \\
 Z_1 &= \frac{1}{i\omega C_1}, & C_1 &= \frac{\varepsilon_{11}4l\bar{w}}{2\bar{h}}, & Z_2 &= \frac{1}{i\omega C_2}, & C_2 &= \frac{\varepsilon_{11}4wh}{2l}.
 \end{aligned} \tag{34}$$

In Eq. (34), k_{15} is an electromechanical coupling factor, ω_0 the thickness-shear resonant frequency for shorted receiving electrodes ($Z_L = 0$) as predicted by the zero-dimensional theory, C_1 and C_2 the static capacitance of the driving and receiving portions, and Z_1 and Z_2 the impedance of the two portions. As a numerical example, for PZT-5H, we have [6].

$$\begin{aligned}
 \rho &= 7500 \text{ kg/m}^3, & c_{11} &= 12.6, & c_{33} &= 11.7, & c_{44} &= 2.30, \\
 c_{12} &= 7.95, & c_{13} &= 8.41 \times 10^{10} \text{ N/m}^2, \\
 c_{66} &= (c_{11} - c_{12})/2, \\
 e_{15} &= 17.0, & e_{31} &= -6.5, & e_{33} &= 23.3 \text{ C/m}^2, \\
 \varepsilon_{11} &= 1700\varepsilon_0, & \varepsilon_{33} &= 1470\varepsilon_0, & \varepsilon_0 &= 8.854 \times 10^{-12} \text{ farads/m}.
 \end{aligned} \tag{35}$$

Material damping can be included by allowing c_{pq} to assume complex values [12]. In our case, c_{44} will be replaced by $c_{44}(1 + iQ^{-1})$, where c_{44} and Q are real and the value of Q for ceramics is usually on the order of 10^2 to 10^3 [12]. In the following, we will fix the value of Q to be 10^2 in our calculations.

The transforming ratio $|\bar{V}_2/\bar{V}_1|$ as a function of the driving frequency ω is shown in Fig. 3. It is seen that when ω is close to the resonant frequency ω_0 , the transforming ratio assumes maximum, indicating that the transformer is a resonant device working only at (or close to) a particular frequency. We note that in general the load impedance Z_L is also a function of ω . The form of this function depends on the specific structure of the loading circuit. When the loading circuit is essentially capacitive, Z_L is pure imaginary and Z_2/Z_L is a real number.

$|\bar{V}_2/\bar{V}_1|$ versus the aspect ratio l/\bar{h} (the length of the receiving portion over the thickness of the driving portion) is plotted in Fig. 4. An essentially linearly increasing behavior is observed. Fig. 4 exhibits

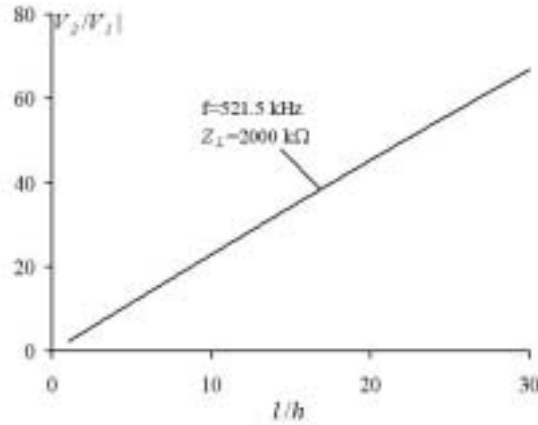


Fig. 4. Transforming ratio versus aspect ratio.

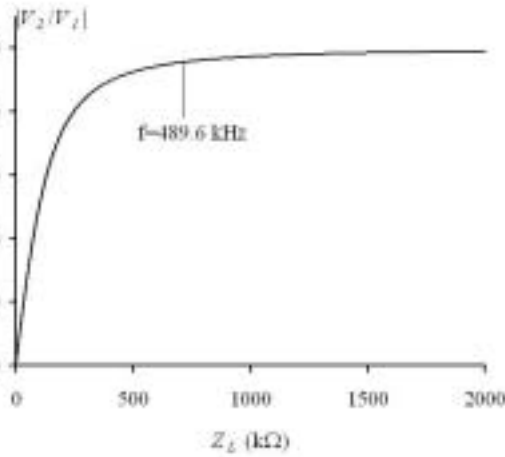


Fig. 5. Transforming ratio versus load.

the voltage raising ability of this transformer from a different angle. Clearly, for large aspect ratios or long and thin transformers, high voltage output can be achieved. The zero-dimensional equations are particularly suitable for long and thin transformers with almost uniform fields. The dependence of the transforming ration on l/\bar{h} can also be seen from the factor of l/\bar{h} in Eq. (33)₁.

It can be concluded from inspection of Eq. (33)₁ that for small Z_L or almost shorted receiving electrodes, $|\bar{V}_2/\bar{V}_1|$ as a function of Z_L is linear in Z_L . For very large Z_L or almost open receiving electrodes, the transforming ratio approaches a constant (saturation). We note from Eq. (33)₂ that the output current \bar{I}_2 has such a dependence on Z_L that when Z is small \bar{I}_2 has a finite value and when Z_L is large \bar{I}_2 approaches zero. This is as expected. $|\bar{V}_2/\bar{V}_1|$ as a function of Z_L is shown in Fig. 5.

The input and output powers of the transformer, in terms of the complex notation, are given by

$$P_1 = \frac{1}{4}(\bar{I}_1\bar{V}_1^* + \bar{I}_1^*\bar{V}_1), \quad P_2 = \frac{1}{4}(\bar{I}_2\bar{V}_2^* + \bar{I}_2^*\bar{V}_2), \tag{36}$$

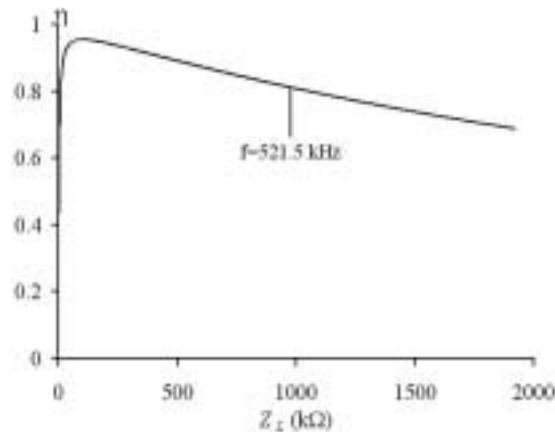


Fig. 6. Efficiency versus load.

where an asterisk means complex conjugate. Then the efficiency of the transformer is defined by

$$\eta = P_2/P_1. \quad (37)$$

It can be concluded that the efficiency as a function of Z behaves as follows. For small loads, η depends on the load linearly. For large loads, η decreases to zero. The efficiency as a function of Z_L is shown in Fig. 6. The behaviors shown in Figs 3–6 for the thickness-shear transformer are qualitatively very similar to the behaviors of the Rosen extensional transformer analyzed in [13].

5. Conclusion

Piezoelectric materials can be used to make thickness-shear high voltage piezoelectric transformers. Analytical solutions for the forced vibration characteristics of a thickness-shear transformer are obtained. The solutions show that high voltage output can be achieved using large aspect ratios. The zero-dimensional equations for a piezoelectric parallelepiped are shown to be effective in the analysis of the transformer.

References

- [1] C.A. Rosen, *Ceramic Transformers and Filters*, Ph.D. Thesis, Syracuse University, 1956.
- [2] T. Zaitso, O. Ohnishi, T. Inoue, M. Shoyama, T. Ninomiya, F. C. Lee and G.C. Hua, *Piezoelectric transformer operating in thickness extensional vibration and its application to switching converter*, IEEE PESC Record, 1994, pp. 585–589.
- [3] K. Nakamura and K. Kumasaka, *Lame-mode piezoelectric resonator and transformers using LiNbO₃ crystals*, Proc. IEEE Ultrasonics Symp., 1995, pp. 999–1002.
- [4] N. Wakatsuki, M. Ueda and M. Satoh, Low-loss piezoelectric transformer using energy trapping of width vibration, *Jpn. J. Appl. Phys.* **32** (1993), 2317–2320.
- [5] J.S. Yang and W. Zhang, A thickness-shear high voltage piezoelectric transformer, *Int. J. of Applied Electromagnetics and Mechanics* **10** (1999), 105–121.
- [6] B.A. Auld, *Acoustic Fields and Waves in Solids*, (Vol. 1), John Wiley and Sons, New York, 1973, pp. 357–382.
- [7] D. Salt, *Hy-Q Handbook of Quartz Crystal Devices*, Van-Norstrand and Reinhold, UK, 1987, Chap. 3.
- [8] J.S. Yang, H. Fang and Q. Jiang, Equations for a piezoelectric parallelepiped and applications in a piezoelectric gyroscope, *Int. J. of Applied Electromagnetics and Mechanics* **10** (1999), 337–350.

- [9] H. Cohen and R.G. Muncaster, *The Theory of Pseudo-rigid Bodies*, Springer, New York, 1988.
- [10] H.F. Tiersten, *Linear Piezoelectric Plate Vibrations*, Plenum, New York, 1969.
- [11] R.D. Mindlin, High frequency vibrations of piezoelectric crystal plates, *Int. J. Solids Structures* **8** (1972), 895–906.
- [12] R. Holland and E.P. EerNisse, *Design of Resonant Piezoelectric Devices*, M.I.T. Press, Cambridge, 1968.
- [13] J.S. Yang and X. Zhang, Extensional vibration of a nonuniform piezoceramic rod and high voltage generation, *Int. J. of Applied Electromagnetics and Mechanics* **16** (2002), 29–42.

Copyright of International Journal of Applied Electromagnetics & Mechanics is the property of IOS Press and its content may not be copied or emailed to multiple sites or posted to a listserv without the copyright holder's express written permission. However, users may print, download, or email articles for individual use.